9th Asia-Pacific Conference on Wind Engineering
Auckland, New Zealand
3-7 December 2017

Investigation of the Failure Progression of a 1-Story Gable-Roof Building Subjected to Sustained Wind Speeds

Liezl Raissa E. Tan[1] and Dr. Jaime Hernandez Jr.[1]

[1]Institute of Civil Engineering
University of the Philippines Diliman, 1101 Quezon City, Philippines

Abstract

Failure assessment of buildings were typically done at the onset failure. Onset failure is defined as the set of damages acquired from an initially closed structure that is subjected to severe wind. Studies that considered progressive failure approximates the pressure on the damaged panels as an average of the internal and external pressures. This study investigates the difference in the amount of damage incurred at the onset and the case wherein the damaged building was continuously subjected to a sustained wind speed. Results show that for a 1-story gable-roof building, a substantial deviation on the damage ratio ranging from 1.1% to 6.4% occurs between 30 m/s to 60 m/s.

Introduction

Building failure assessment was conducted by employing a component-based approach in reliability modelling. The failure probabilities were estimated at each identified critical building components by quantifying its probabilistic resistance capacities and subjecting it to increasing deterministic wind speeds.

Vulnerability curves are commonly used as a measure of the total performance of a building across various hazard intensities. The abscissa of a vulnerability curve describes the hazard intensity while its ordinate gives the amount of damage. This study made use of the same measure to quantify the damage incurred across increasing wind speeds. The quantity used to represent the hazard intensity is the local wind speed, while that of the amount of damage is the damage ratio.

Damage ratio is the ratio of the repair cost to the construction cost. This study made use of the cost as the unifying unit to be able to aggregate the amount of damage incurred by various building components into one quantity that represents the total damage of a building.

Methodology

The study started with identifying the critical building components where failure is evaluated and their corresponding failure modes. The critical components identified include the roof cover, roof-truss-to-column connections, purlin connections, purlin sections and the window panels.

The failure modes associated with the roof cover include the pull-out and pull-thru capacity of the roof fastener. The pull-out failure mode is the failure of the connection between the roof fastener and the purlin, while the pull-thru failure mode is the failure of the connection between the roof fastener and the roof cover due to tearing of the roof cover.

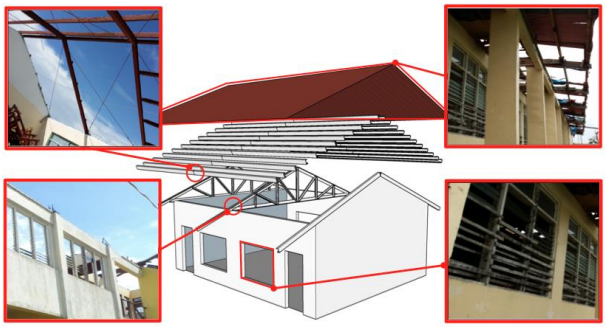

Figure 1.Commonly observed damages in buildings during the post-Yolanda survey.

Roof-truss-to-column connections were typically made of extended longitudinal rebars wrapped around the truss, hence the corresponding failure mode observed in the field is the unbending of the rebars.

Purlins were welded on angle bars that were welded on the truss. Hence the failure mode for the purlin connection is the failure of the weld connection.

Purlin section failure was defined when the fiber yield stress of 248 MPa, which was based from the nominal capacity, was exceeded by the maximum fiber stress from the unsymmetric biaxial bending of the purlin section.

Lastly, failure of the window panel was defined when the local pressure on the window panel exceeds the estimate load resistance.

Resistance capacities of the various identified failure modes were quantified which were based on either material test, existing literature or their nominal design strengths. These are summarized in the table below.

Building Elements	Mean	C.O.V	Distribution
Unbending of rebars	12.28 kN	0.63	Lognormal
Purlin Section	248 MPa	-	Deterministic
Purlin Connection	232.25 kN	0.063	Lognormal
Tek Screw : Pull-Out	538.7 N	0.1	Lognormal
Tek Screw : Pull-Thru	1467.8 N	0.09	Lognormal
Window Panel	2.5 kPa	0.2	Gaussian

Table 1. Summary of resistance capacities.

A wind tunnel test was conducted for the same building of interest. However the damage cases considered were limited to the removal of the window panels. Moreover, pressure measurements were available for one of the exterior rooms of the building as shown in

Figure 2. For these reasons, a numerical modelling was necessitated.

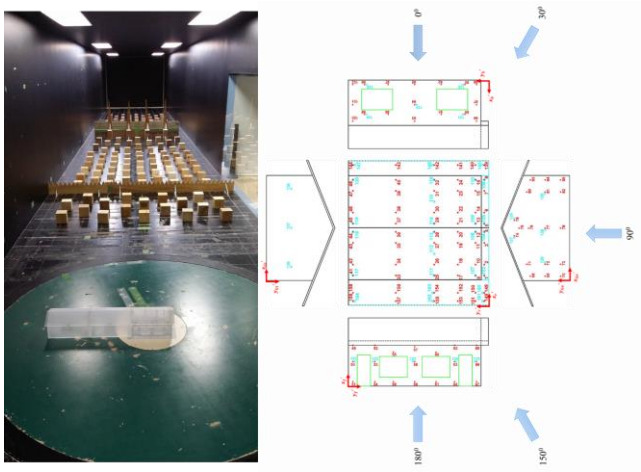

Figure 2. Wind tunnel test set-up.

The numerical modelling employed the computational fluid dynamics to estimate the fluid flow around the building. This was implemented with the use of ANSYS.

The building was modelled in full-scale wherein the enclosure dimensions used were patterned after the dimensions of the test section. A global fine mesh with curvature and proximity refinement was implemented with local sizing of 0.1 m maximum mesh size applied on all the building surfaces and a local inflation layers of 15 layers on all the building surfaces and the ground.

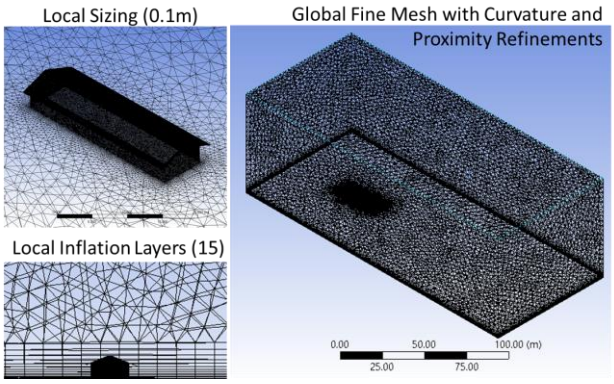

Figure 3. Mesh parameters used in the numerical modelling.

The experimentally developed velocity profile was assigned at the inlet with a turbulence intensity of 10 %. A zero reference average static pressure with 5% pressure blend was assigned at the outlet. The side walls and the top wall of the enclosure were assigned with free-slip wall while the ground and the building surfaces were assigned with a no-slip wall.

The fluid used was an isothermal air following the ideal gas at 25 ^{0}C. The turbulence model used was the Shear Stress Transport Model (SST) employing the Reynold's Averaged Navier-Stokes equations for the numerical method with a convergence criteria of 1×10^{-4} residual of the root-mean-squares.

The results of the numerical model were compared with the wind tunnel test results for cases with no openings, front side windows were opened and all windows were opened. Sample charts plotting the values of the pressure coefficients (*Cp*) against every pressure tap for the case having no openings and for wind directions 0^0, 30^0, and 90^0 are shown in figure 4. The plot of the results from the simulation and the wind tunnel test were superimposed for validation of the model. From these charts, it was concluded that the simulation results are in good agreement with the wind tunnel test results and hence the CFD model is sufficient for the purpose of this study.

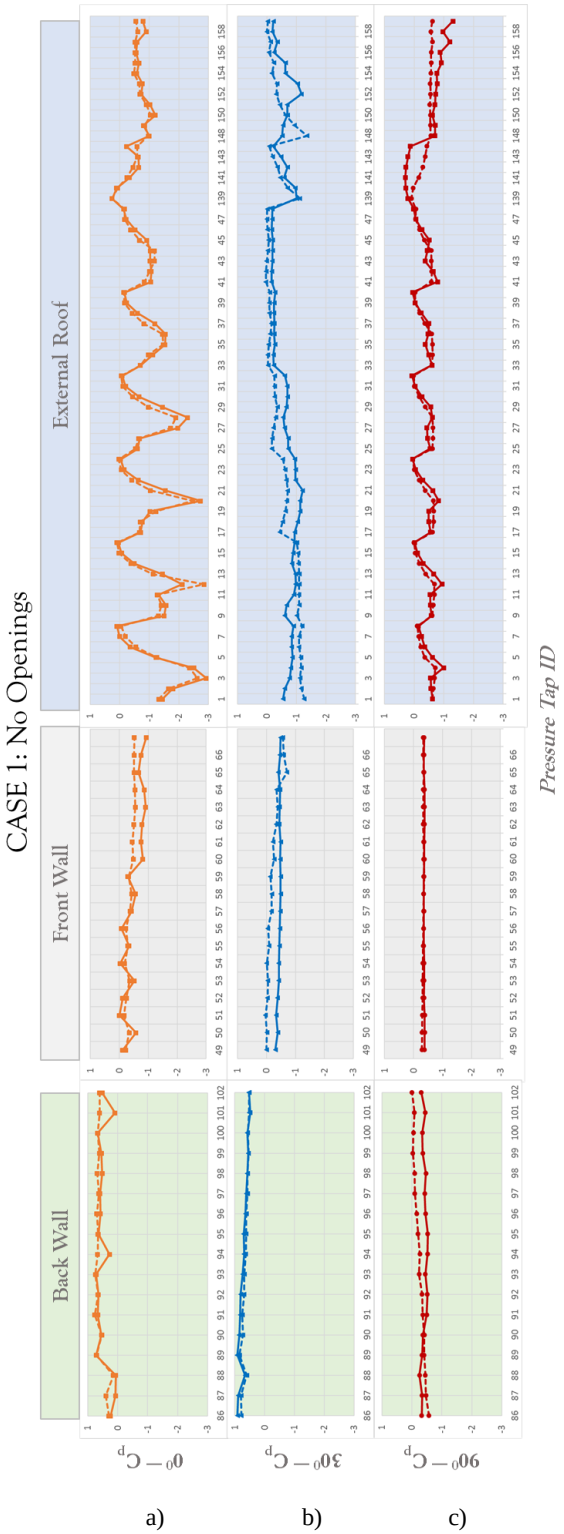

Figure 4. Superimposed plots of the pressure coefficient values against pressure tap ID for the case without openings and for wind directions a) 0^0, b)30^0, and c) 90^0 of the results of the simulation and the wind tunnel test.

After validating the numerical model, the same set of modelling parameters were used to approximate the pressure distribution for partially damaged geometries.

Failure Assessment

The flowchart used in the failure assessment is shown in figure 5. Using the information on the building configuration and dimensions, the critical building components were discretised into building elements. Moreover, linkages across various building components were also generated.

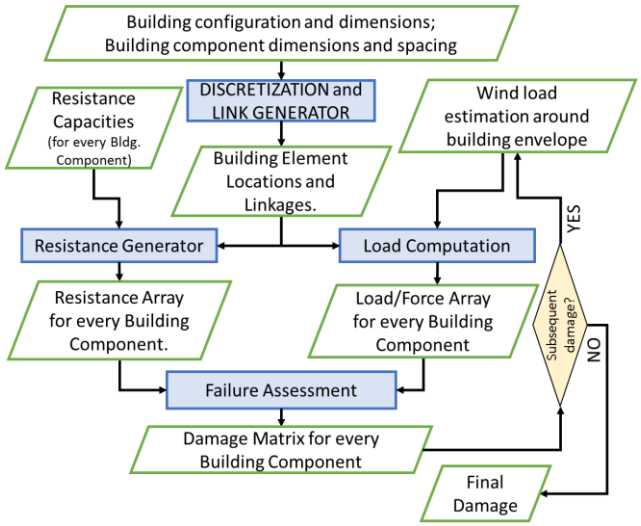

Figure 5. Flowchart of the failure assessment.

Linkages were necessitated since the failure of some components were affected by the failure of other components. This is prominently seen at the roof system, wherein the failure of the overlying components was affected by the failure of the underlying components. Hence, this study sets the direction of the failure propagation to be proliferating upward as illustrated in figure 6.

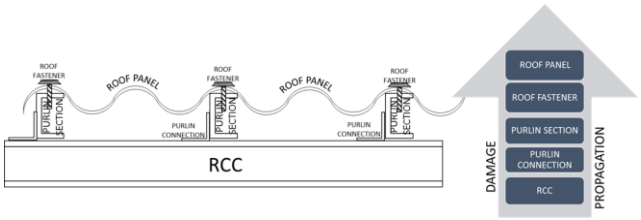

Figure 6. Failure propagation.

Resistance values are then randomly generated at the discretised building elements using the quantified probabilistic parameters of the resistance capacities.

Using the results of the numerical model of the fluid flow around the building envelope, the load at the building elements were computed by transmitting the pressure into equivalent forces at the building elements. The roof system is modelled as frame elements and is loaded with concentrated forces at the locations of the roof fasteners. The concentrated forces represent the equivalent forces of the pressure on the roof panel.

With the resistance values and the corresponding forces quantified at the building elements, the evaluation of the failure then ensues. Failure is defined when the resistance capacity is exceeded by the estimated load.

The result of the failure assessment are damage probabilities at the building component level. In order to aggregate these damage probabilities into one quantity that will represent the total amount of damage for the entire building, cost factors were quantified and incorporated into the process. The cost ratio of the various building components with respect to the cost of the entire building were multiplied with the damage probabilities of the corresponding building components and the summation of which represents the damage ratio of the entire building.

Results and Discussion

The graph in figure 7 shows the superimposed plots of the onset and the final vulnerability curves with the observed damage on similar structure of interest during the typhoon Niña.

The data points from both the simulation and the observed damage were fitted with a modified lognormal cumulative distribution function, which is described in the following equation.

$$\Phi\left(\frac{ln(x - x_{min}) - \mu}{\sigma}\right) * \frac{C_{r\&w}}{CC} \quad (1)$$

Where,
x - wind speed (m/s)
x_{min} - min. considered wind speed (20 m/s)
$\frac{C_{r\&w}}{CC}$ – ratio of the cost of the entire roof and window system to the building construction cost. (19.58%).
μ - median parameter
σ – standard deviation parameter

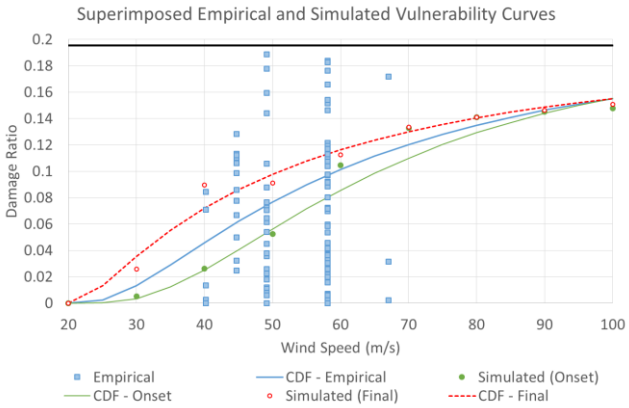

Figure 7. Superimposed vulnerability curves of the onset, final and observed damage.

The curve-fitting parameters are summarized in table 2.

Curve	μ (m/s)	σ (m/s)
Observed	38.47	0.90
Onset	44.70	0.71
Progressive	29.96	1.20

Table 2. Curve-fit parameters for the various vulnerability curves.

The graph shows significant deviation on the damage ratios for wind speeds ranging from 30 m/s to 60 m/s. The deviations on the damage ratios are summarized in table 3.

Wind Speed	DR dev.	Wind Speed	DR dev.
30 m/s	2.10%	70 m/s	0.40%
40 m/s	6.40%	80 m/s	0.30%
50 m/s	4.00%	90 m/s	0.40%
60 m/s	1.10%	100 m/s	0.60%

Table 3. Damage ratio deviations between onset and progressive vulnerability curves across wind speeds.

The T-test results show that both onset and final vulnerability curves can be used to represent the observed damage with the final vulnerability curve offering the closest approximate. Using the

onset vulnerability curve tends to overestimate the damage while the final vulnerability curve underestimates the damage.

Curve	t-Stat	P(T<=t) two-tail	t-critical two-tail
Onset	2.48	0.06	2.57
Progressive	-0.20	0.85	2.57

Table 4. Tabulated values of the t-test for onset and progressive damage relative to the observed damage.

Conclusions

Two vulnerability curves were developed for a one-story gable-roof building using the failure simulation model developed in this study — on-set damage and progressive damage. The empirical curve derived from observed damage data shows good agreement with the simulation results. Moreover, it shows that considering on-set damage only over-estimates the strength of the structure while considering progressive damage in the simulation under-estimates its strength.

Between the two simulated vulnerability curves, the one that resulted from considering progressive damage gives the closest estimate of the damage.

Acknowledgments

The authors would like to acknowledge the collaboration with Kyoto University under the JRapid Project headed by Dr. Kazuyoshi Nishijima in conducting the field survey in Tacloban. The authors would also like to extend their gratitude to Hiroaki Nishimura of the Disaster Prevention Research Institute and Tokyo Polytechnic University represented by Dr. Masahiro Matsui for conducting the material testing and wind tunnel testing, respectively and sharing their test data.

The authors would like to acknowledge the aid provided by Engr. Timothy Acosta and Mr. Jeo Galisim in conducting field surveys in Bicol for the empirical vulnerability curves used in the validation of the result of this study.

The authors would also like to extend their gratitude to Engr. Ebio for providing design plans and bill of quantities used to estimate the damage costs.

References

[1] ANSYS, Inc. (2009). “Introduction to Using ANSYS FLUENT in ANSYS Workbench: Fluid Flow and Heat Transfer in a Mixing Elbow. (Sept. 10, 2009). Tutorial

[2] ARA (Applied Research Associates, Inc.), (2002). Development of Loss Relativities for Wind-Resistive Features of Residential Structures, Version 2.2. *Report for the Florida Department of Community Affairs*.

[3] ASTM Standard E1300-12a (2012). *Standard Practice for Determining Load Resistance of Glass in Buildings*. West Conshohocken, PA: ASTM International.

[4] Cope, Anne D. (2004). “Predicting the vulnerability of typical residential buildings to hurricane damage.” (Doctoral Dissertation). University of Florida.

[5] Dagnew, A., Bitsuamalk, G. and Merrick, R. (2009). Computational evaluation of wind pressures on tall buildings. In: *11th American Conference on Wind Engineering*. [online] Available at: http://iawe.org/Proceedings/11ACWE/11 ACWE- Dagnew.pdf [Accessed 4 January 2015].

[6] Davenport, A. (2007). *Wind Tunnel Testing: A General Outline.* [online] Ontario, Canada. Available at: http://www.blwtl.uwo.ca/User/Doc/Wind%20Tunnel% 20Outline-Web.pdf [Accessed 14 Aug. 2014].

[7] Doguiles, A.E.R. (2015). Failure Modeling of Roof-Truss Supports of Reinforced Concrete Frame Residential Buildings due to Severe Wind. Thesis. University of the Philippines – Diliman, Institute of Civil Engineering.

[8] Goyal, P., Datta, T. and Vijay, V. (2012). Vulnerability of rural houses to cyclonic wind. *International Journal of Disaster Resilience in the Built Environment*, 3(1), pp.20-41.

[9] Kanvinde A. Gomez, I., Kwan Y.K., Grondin, G. (2008). “Strength and Ductility of Welded Joints subjected to Out-of-Plane Bending”. AISC Final Report (July 2008).

[10] Murakami, S. (1990). Computational Wind Engineering. *Journal of Wind Engineering and Industrial Aerodynamics.* 36. pp. 517-538.

[11] Murakami, S. (1993). Comparison of Various Turbulence Models applied to a bluff body. *Journal of Wind Engineering and Industrial Aerodynamics* 46 & 47. Pp. 21-36.

[12] Nishimura H., (personal correspondence April 2015) .roof screw pull-out and pull-through strengths.

[13] Pinelli, J., Gurley, K., Subramanian, C., Hamid, S. and Pita, G. (2008). Validation of a probabilistic model for hurricane insurance loss projections in Florida. *Reliability Engineering & System Safety*, 93(12), pp.1896-1905.

[14] Pita, G., Pinelli, J., Cocke, S., Gurley, K., Mitrani-Reiser, J., Weekes, J. and Hamid, S. (2012). Assessment of hurricane-induced internal damage to low-rise buildings in the Florida Public Hurricane Loss Model. *Journal of Wind Engineering and Industrial Aerodynamics*, 104-106, pp.76-87.

[15] Stathopoulos, T. (1997). Computational wind engineering: Past achievements and future challenges. *Journal of Wind Engineering and Industrial Aerodynamics* 67&68. Pp. 509-532.

[16] Unanwa, C., McDonald, J., Mehta, K. and Smith, D. (2000). The development of wind damage bands for buildings. *Journal of Wind Engineering and Industrial Aerodynamics*, 84(1), pp.119-149.

[17] TPU. (2007). “Aerodynamic database for isolated low-rise buildings”.(http://www.wind.arch.t-kougei.ac.jp/info_center /windpressure////)

[18] Zhang, S., Nishijima K., Maruyama T. (2014). “Reliability-based modeling of typhoon induced wind vulnerability for residential buildings in Japan”. Journal of Wind Engineering and Industrial Aerodynamics. 124. pp. 68-81.